

**PERLECAN/HSPG2 DEFICIENCY ENHANCES BMP2 EFFECT ON
BONE MATRIX MINERALIZATION**

by

Nadia Lepori-Bui

A thesis submitted to the Faculty of the University of Delaware in partial fulfillment of the requirements for the degree of Master of Science in Biological Sciences

Summer 2012

Copyright 2012 Nadia Lepori-Bui
All Rights Reserved

**PERLECAN/HSPG2 DEFICIENCY ENHANCES BMP2 EFFECT ON
BONE MATRIX MINERALIZATION**

by
Nadia Lepori-Bui

Approved: _____
Catherine B. Kirn-Safran, Ph.D.
Professor in charge of thesis on behalf of the Advisory Committee

Approved: _____
Randall L. Duncan, Ph.D.
Chair of the Department of Biological Sciences

Approved: _____
George H. Watson, Ph.D.
Dean of the College of Arts and Sciences

Approved: _____
Charles G. Riordan, Ph.D.
Vice Provost for Graduate and Professional Education

ACKNOWLEDGMENTS

First and foremost, I have to thank my advisor, Dr. Catherine Kirn-Safran, for her kindness and guidance over the past two years. She has taught me so much, and I feel extremely lucky to have had the opportunity to work in her lab. She was a calming and patient mentor, which was much appreciated when experiments did not always turn out well. She encouraged me to submit abstracts for several conferences and helped me find opportunities to enrich my graduate school career. With her help, I was invited to give a podium presentation at ORS, which was an invaluable experience. She was always there with both reassuring words and nudges when I needed them. I sincerely thank her for being the perfect mentor for me.

I'd like to especially thank my committee members, Dr. Randy Duncan and Dr. Erica Selva. Dr. Duncan always had great insights as well as challenges at committee meetings. He also helped me prepare for my podium presentation at ORS, and I felt very honored when he looked at my cells one day. I also thank him for his compassion and real interest in his students' lives and well-being. Dr. Selva brought an entirely different but equally helpful perspective to my project, and always had a friendly smile to share. I'm extremely grateful to her for being on my committee.

Many thanks go to Dr. Kirk Czymmek for his help in optimizing my perlecan immunostaining protocol. Sincere thanks to Jim Farmer, who always fixed everything and essentially kept the whole department running smoothly. Particular thanks go to Doreen Anderson, Tina Fontana, and Betty Cowgill for always going above and beyond in helping me and the other grad students, from scheduling our meetings to

helping us organize our paperwork and theses. I am overwhelmed by all you do for us all the time.

I owe a huge thank you to the members of Dr. Kirn-Safran's lab, both past and present, who all helped me so much. Many thanks to Padma for all the help with QPCR, figuring out primers, and dissection work. Huge thanks to Dylan for his help with literally everything, and having my back and my cell culture all the time. To Dr. Kerry Falgowski, for her help with the osteocalcin ELISA, for teaching me how to use a multichannel pipette, and for taking care of business, a massive thanks. To Dr. Billy Thompson, for teaching me many new techniques, including proper sterile cell culture, and showing me the ropes when I first arrived, a million thanks.

A huge thanks goes out to TKB and my grad student family, particularly Tracy, Lauren, Kerri, Brandy, Sen, Sona, Miho, and Kaitlin, for always being there for me with friendship, moral support, and often, food. I will always remember the time spend learning, studying, laughing, crying, feasting, and succeeding alongside you as the best part of graduate school. I would not have made it without you all.

And of course, all the thanks in the world go to my parents, Anh-Dung Bui and Dolores Lepori, for tirelessly and unfailingly believing I could succeed. Michelle, the best sister in the world, I thank for not distracting me *too* much while I was writing, and for all the jokes and pep talks. I'm grateful to Maggie, my best flower friend, for always being less than a Skype call away. I'm thankful to Alex, my boyfriend, for his unending patience with me. My family and friends' love and support have carried me through all the ups and downs of the last two years, as they have for my whole life. There is little else to add.

Lastly, I dedicate this thesis to my grandfather, Bruno Lepori, *con tanto amore*.

TABLE OF CONTENTS

LIST OF TABLES	vii
LIST OF FIGURES	viii
ABSTRACT	ix

Chapter

1. INTRODUCTION	1
1.1 Perlecan	1
1.2 Long Bone Formation and Mineralization	3
1.3 Bone Morphogenetic Protein 2.....	7
1.4 Perlecan-Deficient Mouse Model.....	7
1.5 Experimental Approach.....	12
2. MATERIALS & METHODS	15
2.1 Animal Care and Handling	15
2.2 Primary MEF Extraction	15
2.3 Primary Osteoblast Extraction.....	16
2.4 Cell Culture Conditions, Differentiation/Mineralization assays	16
2.5 Immunostaining for Perlecan	17
2.6 Reverse Transcriptase-PCR Analysis.....	18
2.7 ELISA Analysis of Media	18
3. RESULTS	19
3.1 Differentiation/Mineralization Results in MEFs	19
3.1.1 Expression of Perlecan by Primary WT and Perlecan- Deficient MEFs	19
3.1.2 Differentiation of MEFs with BMP2.....	21
3.1.3 Mineralization Assay in Differentiated MEFs	21
3.1.4 Analysis of Mineralization Marker Gene Expression in Perlecan-Deficient MEFs Relative to WT.....	24
3.1.5 Perlecan-Deficient MEFs Secrete Elevated Levels of Osteocalcin Relative to WT During Mineralization.....	25

3.2 Mineralization Data in Primary Osteoblasts.....	27
4. DISCUSSION.....	29
REFERENCES	39
Appendix	
PERMISSION LETTER... ..	43

LIST OF TABLES

Table 1.	Summary of percent differences in phenotypic properties of adult mouse bones, perlecan-deficient bones compared to WT.	12
Table 2.	Osteocalcin levels secreted into the media of WT and mutant MEFs culture in the presence or absence of BMP2.	27

LIST OF FIGURES

Figure 1.	The structure of perlecan.....	2
Figure 2.	Schematic of endochondral ossification for the formation and growth of long bones. (Cummings 2006).....	6
Figure 3.	Skeletal analysis of WT and perlecan-deficient newborn pups.	9
Figure 4.	A. Immunostaining and von Kossa staining of embryonic day 18.5 mouse growth plates.	10
Figure 5.	Perlecan immunostaining of WT and perlecan-deficient MEFs <i>ex vivo</i>	20
Figure 6.	Alkaline phosphate staining is elevated in perlecan-deficient MEFs treated with BMP2 compared to treated WT MEFs.	22
Figure 7.	Von Kossa staining of WT and perlecan deficient MEFs only shows mineral deposition in the perlecan-deficient cells treated with BMP2.	23
Figure 8.	Quantitative real time PCR data for selected osteogenesis markers reveals significant upregulation in BMP2-treated perlecan-deficient cells relative to treated WT cells..	25
Figure 9.	Perlecan-deficient and WT osteoblasts at day 21 of culture under osteogenic conditions exhibit similar patterns of Alizarin red staining.	28
Figure 10.	Working model of perlecan-deficiency's effect on bone development in the growth plate.	32
Figure 11.	In the WT growth plate in developing bone, perlecan (green slashes) is expressed in the growth plate, periosteum, and bone marrow, where it serves to regulate osteogenesis for proper bone formation.	33

ABSTRACT

Perlecan/HSPG2 is a heparan-sulfate proteoglycan abundantly expressed in all basement membranes of the body and in the extracellular matrix of cartilage. It holds important regulatory functions during endochondral ossification, as is evidenced by the severe skeletal dysplasias that result from lethal null mutations of the *Hspg2* gene. Specific perlecan gene mutations that result in reduced levels of functional protein expression are non-lethal in humans and mice, and result in Schwartz-Jampel syndrome (SJS) in humans. SJS patients exhibit a milder range of skeletal abnormalities including shortened long bones and disorganized growth plate. Perlecan expression begins in the growth plate at the onset of endochondral ossification, but drops completely upon mineralization of the developing bone matrix at the chondro-osseous junction. In perlecan-deficient mouse growth plates, the enlarged and disorganized growth plates have also been associated with abnormal matrix mineralization. Based on these observations, I hypothesize that perlecan's presence in the developing bone serves as a modulator of osteogenesis to ensure endochondral ossification occurs correctly, and that it does this through the attenuation of growth factor signaling via heparin sulfate chains. When perlecan is absent or deficient in the matrix, enhanced heparan-binding growth factor signaling is allowed to occur, resulting in widespread differentiation of osteoprogenitors and abnormal shape and progression of the growth plate. To test this hypothesis, I use an in vitro cell culture system of primary mouse embryonic fibroblasts (MEFs) derived from both WT and perlecan-deficient mice to determine if differentiation and mineralization potential are

affected by perlecan deficiency. Perlecan-deficient MEFs were found to differentiate and mineralize, as visualized by alkaline phosphatase and von Kossa staining, respectively, both earlier and to a greater extent than their WT counterparts. Several key markers of mineralization were highly upregulated in perlecan-deficient cells relative to WT cells. Levels of osteocalcin, an important marker of bone mineralization, secreted by osteoblasts was also elevated in the media from perlecan-deficient vs. WT cells. Though much remains to be uncovered about the mechanism of how perlecan contributes to the maintenance of proper bone matrix structure, these studies clearly demonstrate a role for perlecan in the modulation of growth factor activity during osteogenesis.

Chapter 1

INTRODUCTION

1.1 Perlecan

Perlecan is a large, extracellular heparan-sulfate proteoglycan (Figure 1). Its protein core (~400kDa) consists of five distinct domains characterized by their homology to other cell adhesion molecules (Knox and Whitelock 2006). The N-terminal domain I contains three serine-glycine-aspartic acid sequences where heparan sulfate (HS) chains can attach. Internal protein modules near these sites enhance the attachment of heparan sulfate over other glucosaminoglycans (GAG) such as chondroitin sulfate during protein modification in the ER, though they can occasionally attach as well (Whitelock and Iozzo 2005). Domain V also contains a single GAG attachment site, and is made up of a combination of laminin motifs and epidermal growth factor (EGF)-like repeats. Domain II contains three low density lipoprotein (LDL) receptor-like motifs, domain III contains motifs with homologous with laminin A, and domain IV contains 14 repeats of IgG-like motifs homologous to those in neural-cell adhesion molecule (N-CAM) (Kirn-Safran et al. 2004).

Perlecan is expressed in all basement membranes of the body, in the vasculature, and in the bone lacuno-canalicular system (LCS) (Thompson et al. 2011). Its various domains and HS chains allow it to interact with numerous basement membrane components, including laminin, type IV collagen, fibronectin, entactin, and nidogen, contributing to the structure and stability of the membrane (Jiang and Couchman 2003, Knox and Whitelock 2006). Perlecan is also highly expressed in

developing cartilage and the growth plates. Perlecan expression begins at embryonic day 10.5 with the onset of endochondral ossification, a process in which it is a key regulator. The mechanism by which perlecan regulates this process is not well understood, but other than its scaffolding properties, perlecan's ability to interact with growth factors through its HS chains has been the most widely studied (Whitelock and Iozzo 2005).

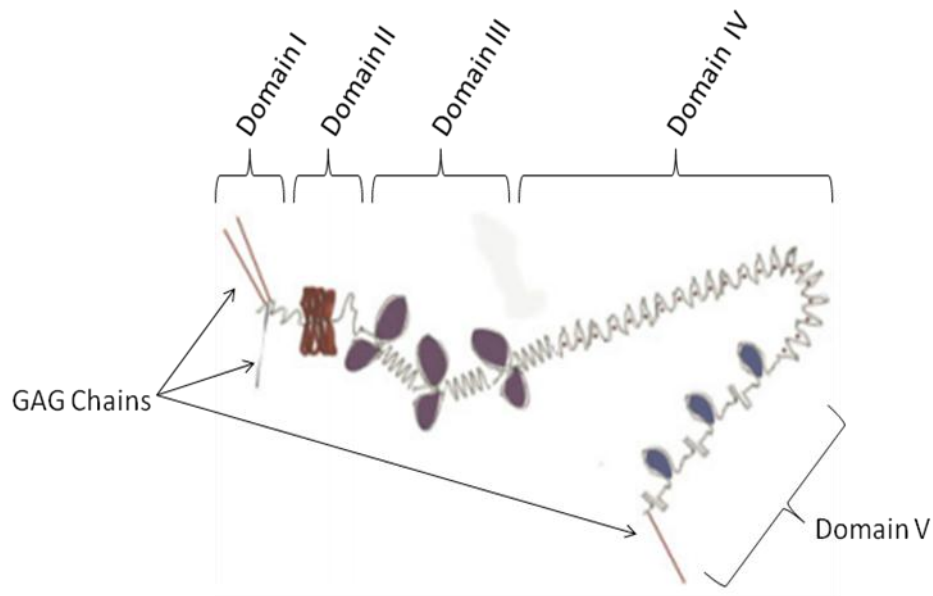


Figure 1. The structure of perlecan. Perlecan is comprised of five distinct, modular domains. Domains I and V includes SGD GAG attachment sequences.

1.2 Long Bone Formation and Mineralization

Endochondral ossification (EO) is the process of bone formation for long bones (Figure 2) (Olsen, Reginato and Wang 2000). Initially, a hyaline cartilage “blueprint” of the bone is laid down by chondrocytes in the limb buds (Figure 2A). In the diaphysis, or the middle of the bone shaft, the chondrocytes grow and mature, laying down the matrix. In the center of the diaphysis, the chondrocytes differentiate terminally then begin to undergo hypertrophy, and the hyaline cartilage becomes calcified. The embedded, terminally differentiated chondrocytes then undergo apoptosis, forming a cavity which becomes the primary ossification center and the future medullary cavity (Figure 2B). Then, vascular invasion begins, bringing blood vessels, osteoblasts, and osteoclasts into the cavity of the calcified cartilage matrix (Ishijima et al. 2012). The perichondrium which surrounds the diaphysis also becomes vascularized, and turns into the periosteum as osteoblasts lay down and mineralize a compact bone collar around the diaphysis (Olsen et al. 2000). Bone formation continues from the primary center as osteoclasts dissolve the calcified cartilage scaffold and osteoblasts replace it with bone matrix (Figure 2C). Osteoblasts that get embedded in the bone matrix as it is formed and mineralizes differentiate into osteocytes and are maintained in the LCS (Thompson et al. 2011). The new bone grows in length through the differentiation and apoptosis of the chondrocytes in the hypertrophic zone, and actively dividing chondrocytes in the proliferative zone supply these cells continually during the growth phase. Secondary centers of ossification also form in the epiphyses located at the ends of the bones, and cancellous, or woven, bone forms from there towards the two growth plates (Figure 2D). In humans, these epiphyseal growth plates will not fuse until after adolescence. Eventually, all the

original cartilage is replaced by bone matrix except at the ends of the epiphyses, where a layer of articular cartilage remains (Figure 2E) (Olsen et al. 2000).

Endochondral ossification is a complex, multistep process dependent on several factors to ensure it occurs correctly (Cohn 2001). First, chondrogenesis and the laying down of the cartilage matrix must occur in a well regulated fashion, as abnormalities in this original matrix will lead to abnormal bone architecture. Vascular invasion is critical as it brings the cells essential for the next step of EO, the osteoclasts and osteoblast precursors (Ishijima et al. 2012). All of these processes are driven by appropriate spatial and temporal expression and distribution of differentiation factors responsible for the induction of specific signaling pathways. Any mutations in the signaling molecules or their cognate receptors can upset the progression of EO and result in abnormal bone formation. Osteoblast activity following vascularization of the periosteum is the first step in the formation of the bone matrix. Osteogenesis imperfecta (OI) is a skeletal dysplasia that can arise from any mutation in the genes that encode procollagen type I or any of the chaperone proteins involved in post-translational modification of collagen type I (Kelley et al. 2011). Procollagen chains produced from the mutated gene do not undergo proper fibrillogenesis because they cannot form triple helices or crosslink with one another, resulting in improper mineralization of the bone matrix. In its mildest form, OI patients have weak bones with low bone mineral density (BMD) which are highly susceptible to fractures without trauma. In its most severe form, bones cannot form at all and the disease is perinatally lethal (Steiner, Pepin and Byers 2005). Once the bone matrix is laid down, the osteoblasts deposit nucleation vesicles along the collagen I fibers and mineralization occurs at a normal rate. If the functions of the bone

remodeling system are disrupted, however, such as in patients with osteopetrosis, mineralization becomes unbalanced as well. Under this condition, although osteoblasts are fully functional, osteoclasts do not resorb bone in conjunction with the osteoblasts' activity (Sobacchi et al. 2007). Osteopetritic bone is denser with increased BMD, and complications arise from decreased bone material property and bone marrow space (Sobacchi et al. 2007). The process of calcification is also dependent on the extracellular environment, and when the normal components or structure of the extracellular environment is disrupted by mutation, abnormal mineralization ensues. Interestingly, both defects leading to hypo- and hypermineralization of the skeleton often lead to smaller stature and are associated with increased bone fragility (Frattini et al. 2007, Rodgers et al. 2007).

Perlecan's presence in the developing cartilage matrix but not in bone matrix suggests that it regulates earlier stages of osteogenic differentiation during EO. Its expression is highest in the pericellular space of prehypertrophic and hypertrophic chondrocytes and in the perichondrium (Kirn-Safran et al. 2004) as well as our WT immunostaining images). When the perlecan gene is knocked out, the mutation is embryonic lethal in mice and humans. Perlecan-null embryos display severe skeletal dysplasias including very short stature and shortened long bones, and altered arrangement of the cells in the hypertrophic zone and growth plate that result in embryonic or perinatal death (Arikawa-Hirasawa et al. 1999, Costell et al. 1999). In humans, perlecan-null mutations give rise to a syndrome called dissegmental dysplasia, Silverman-Handmaker type (DDSH), which results in this severe and lethal phenotype. Individuals with DDSH lack perlecan in all expressing tissues including basement membranes, and lethality is due to developmental complications unrelated to

bone malformations (Rodgers et al. 2007). Schwarz-Jampel Syndrome (SJS) is another skeletal disease caused by reduced amounts of perlecan secreted into the cartilage (Rodgers et al. 2007). SJS is characterized by milder symptoms than DDSH which correlate to the amount of perlecan found in the matrix of these patients. These observations indicate that perlecan's presence in the developing bone is vital for the regular patterning of cartilage matrix, which eventually is essential for the regulation of osteogenesis and normal architecture of the skeleton.

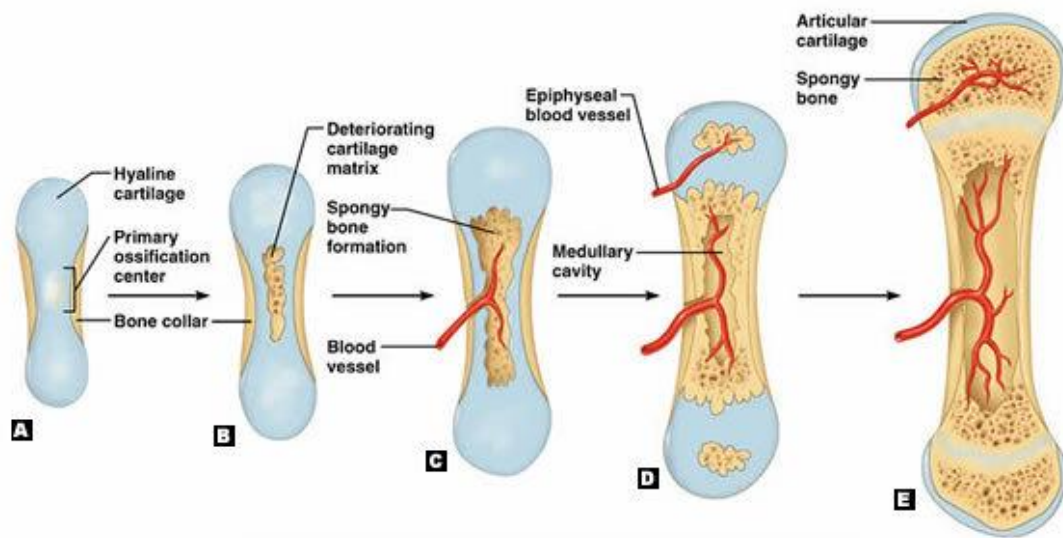


Figure 2. Schematic of the major steps involved in endochondral ossification, for the formation and growth of long bones. (Cummings 2006)

1.3 Bone Morphogenetic Protein 2

Bone Morphogenetic Protein 2 (BMP2) is part of the BMP subgroup in the transforming growth factor-beta (TGF β) superfamily of growth factors (Chen, Zhao and Mundy 2004). It has many target tissues throughout the body and plays important roles during early development, such as in embryonic dorsal-ventral patterning and limb bud formation (Tsumaki and Yoshikawa 2005), as well as bone formation and bone remodeling. In bone formation, BMP2 acts on undifferentiated mesenchymal stem cells to commit them to become osteoprogenitor cells, and then drives those cells towards becoming osteoblasts (Katagiri et al. 1994). Once they are terminally differentiated, however, osteoblasts' sensitivity to BMP2 decreases (Rosen 2012). BMP2 has been used *in vitro* to induce osteoblast differentiations based on the *in vivo* observation that it caused ectopic bone formation when implanted into muscle tissue (Yamaguchi, Komori and Suda 2000).

1.4 Perlecan-Deficient Mouse Model

A viable, perlecan-deficient mouse model was developed by Rodgers et al. to mimic the phenotype of SJS patients (Rodgers et al. 2007). Since the perlecan-null mutation is lethal, the researchers used a gene targeting approach to decrease the amount of extracellular perlecan in the mice's cartilage. A point mutation inserted in exon 36 did not produce the desired phenotype, so a neomycin resistance selection cassette was inserted into intron 36 in the mutant mice. This genetic alteration induced altered transcription of perlecan/HSPG2. Production of a truncated transcript

and decreased levels of full-length transcript resulted in reduced amounts of functional protein produced by these mutant cells (Rodgers et al. 2007).

As mentioned previously, perlecan-deficiency in the developing cartilage results in dwarfism and shortened long bones (Figure 3). The mutant mice also have misshapen ribs and sterna, and flattened faces and eyes. PIn immunostaining in E18.5 wild type (WT) and perlecan-deficient mouse bones reveals strong pericellular signal in the WT, but barely detectable extracellular signal in the developing mutant bone (Figure 4A, compare top to bottom panels). The perlecan that is stained in the mutant bones seems to be mostly retained intracellularly, and co-localizes with the ER marker BiP (Figure 4A, right panels). In both genotypes, perlecan expression ceases completely at the chondro-osseous junction. Collagen X staining shows an expanded and disorganized hypertrophic zone in the perlecan-deficient bones compared to WT bones (Figure 4B, left panels). When compared to von Kossa staining of adjacent sections, the perlecan-deficient bones display widened hypertrophic zones associated with early and abnormal mineralization not seen in the WT bones (Figure 4B, right, red arrows).

Adult perlecan-deficient mice also have skeletal properties reminiscent of SJS patients' symptoms. X-ray analysis demonstrated that at mid-shaft, the cross sectional cortical thickness of perlecan-deficient mouse bones is significantly increased (Table 1) compared to WT (Lowe et al. 2012). Micro-CT data analysis reveals increased BMD in both male and female perlecan-deficient bones compared to WT (Table 1). From mechanical tests, the perlecan-deficient mouse bones are in general more rigid due to their increased BMD and have greater ultimate force measurements relative to WT bones (Table 1) (Lowe et al. 2012). Of particular note is the observation from

transmission electron microscope (TEM) imaging of cortical osteocytes in long bones of perlecan-deficient mice, which show a significant decrease in the pericellular space of these cells in the LCS compared to WT cells (Thompson et al. 2011). Perlecan presence in the pericellular space of osteocytes suggests an important function in the maintenance of LCS integrity, perhaps by inhibiting mineralization in this space.

Though this mouse model is not a perfect genetic match for all cases of SJS, it mimics the phenotype of decreased perlecan secretion in the cartilage matrix and the resulting growth plate defects. Hence this model is a good tool for studying the effects of perlecan-deficiency during bone development.

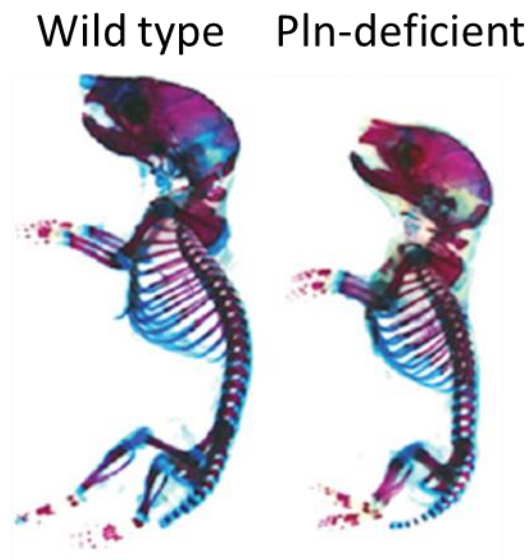


Figure 3. Skeletal analysis of WT and perlecan-deficient newborn pups. Alizarin red S and Alcian blue stains reveal decreased size and thickened and irregular long bones in the perlecan mutant pups compared to WT pups (adapted from Rodgers et al., 2007).

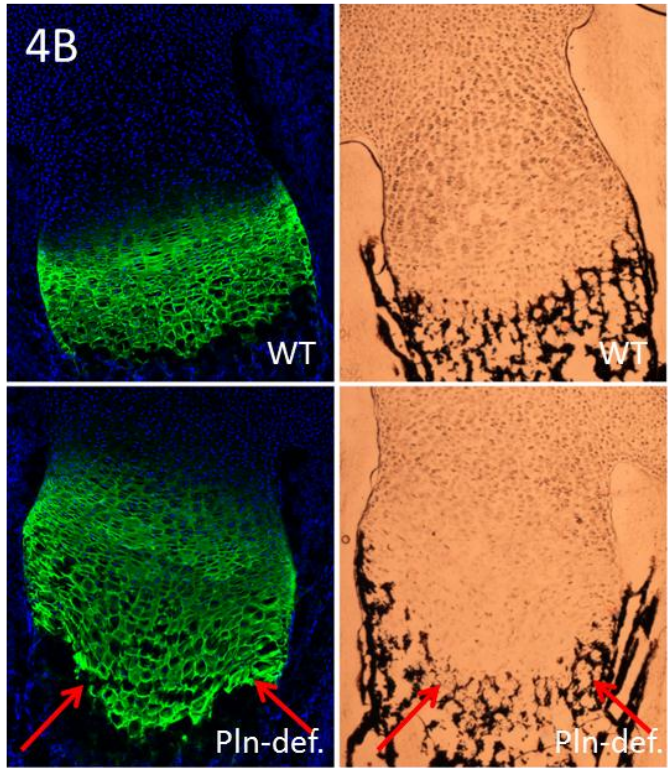
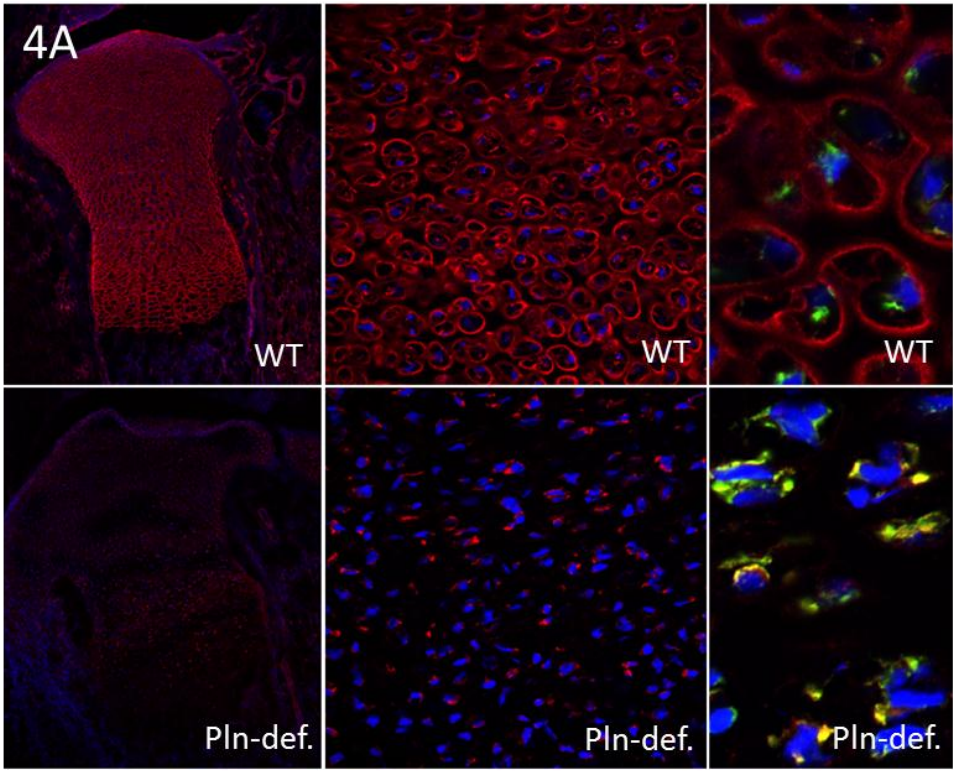


Figure 4. A. Immunostaining and von Kossa staining of embryonic day 18.5 mouse growth plates. Top panels are WT and bottom panels are perlecan-deficient. Perlecan is stained in red and BiP is in green. B. Collagen X is stained in green on the left. Blue is nuclear stain. The right panels show a von Kossa stain for mineralization (adapted from Lowe et al., under revisions). Arrows indicate abnormal mineralization in the hypertrophic zone in the perlecan-deficient growth plate.

Table 1. Summary of percent differences in phenotypic properties of adult mouse bones, perlecan-deficient bones compared to WT. Data are analyzed from micro-CT and X-ray measurements, and asterisks signify statistically significant P-values (Lowe et al. 2012).

	Cortical Area	Bending Rigidity	Ultimate Force	Young's Modulus	Bone Mineral Density
Pln-def. vs. WT, males	+12%*	+13.5%	+32.9%*	+5.3%	+8.3%*
Pln-def. vs. WT, females	+29%*	+125.5%*	+75.6%*	+55.2%*	+9.1%*

1.5 Experimental Approach

In short, perlecan's presence in the developing cartilage starting at embryonic day 10.5 and in the perichondrium and periosteum plays a major role in determining proper bone patterning and development, as is evident from the dysplasias of perlecan-deficient mice. Furthermore, its expression ceases immediately upon mineralization at the osteo-chondrous interface in developing bone. Perlecan carries up to four HS chains, which can modulate growth factor activity. Therefore, I hypothesize that perlecan's presence in the developing bone serves to modulate the process of endochondral ossification by attenuating the terminal differentiation of osteoprogenitor cells through regulation of growth factor signaling.

To test this hypothesis, a cell culture system was developed to compare the differentiation and mineralization potentials of perlecan-deficient and WT cells. Primary mouse embryonic fibroblasts (MEFs) were isolated and cultured under mineralization conditions in the presence of the heparan sulfate growth factor BMP2

to stimulate osteogenesis. A system of primary calvarial osteoblasts was also generated. Three specific aims with subhypotheses are outlined as follows to direct the work with primary cell cultures:

1. To determine if perlecan deficiency affects the *ex vivo* mineralization potential of osteoblast precursors in the presence of the differentiation factor BMP2.
 - Subhypothesis: Perlecan deficiency in primary MEF leads to elevated differentiation potential, and subsequently to elevated mineralization potential, relative to WT cells in culture.

2. To identify differences in the expression of markers of osteogenesis and mineralization in WT and perlecan-deficient primary MEFs undergoing osteogenesis:
 - Subhypothesis: In differentiating osteoprogenitors, markers of mineralization will be upregulated in perlecan-deficient cells relative to WT cells, but in committed osteoblasts, there will not be a difference in gene and protein expression of mineralization markers.

3. To determine if perlecan deficiency has an effect on the mineralization potential of primary osteoblasts in culture.
 - Subhypothesis: Perlecan deficiency in an *ex vivo* system of primary osteoblasts, where regulation of differentiation factors by the ECM has

already taken place and periosteal influence is absent, will not have a pronounced effect on already committed osteoblasts, and WT and perlecan-deficient osteoblasts isolated from calvaria will not show distinct phenotypes when cultured under osteogenic conditions.

Chapter 2

MATERIALS & METHODS

2.1 Animal Care and Handling

All animal handling experiments and animal care were in accordance with the University of Delaware Institutional Animal Care and Use Committee approved guidelines.

2.2 Primary MEF Extraction

Primary MEFs were isolated from day 13.5 embryos from both WT and hypomorphic mouse litters. Individual embryos were dissected away from the uterine horn and rinsed in 1X phosphate-buffered saline (PBS). The heads, tails, and viscera were removed and cleaned. The carcasses were finely minced with forceps and incubated in trypsin/EDTA for 10 minutes at 37°C. Cells were seeded onto prepared gelatinized, 10-cm plates in complete media made of Dulbecco's Modified Eagle Medium (DMEM), (Invitrogen, San Francisco, CA), 10% (v/v) fetal bovine serum (FBS), (Hyclone, Logan, UT), 2mM L-glutamine (Invitrogen), 10^{-4} M β -mercaptoethanol (Sigma-Aldrich, St. Louis, MO), and 50 μ g/mL penicillin and streptomycin (Pen/Strep), (Hyclone). Media was changed every 2 to 3 days and cells were subcultured at confluence.

2.3 Primary Osteoblast Extraction

Primary osteoblasts were isolated from the calvaria of 3-5 day old WT and hypomorphic pups. On day 1, the calvaria were dissected from 5 to 10 pups. The cranial sutures and surrounding tissues were removed, and then the surfaces cleaned under a microscope in 1X PBS. The calvarial halves were placed in complete media of DMEM (Invitrogen) with 10% FBS (Hyclone) and 1% Penn/Step overnight at 37°C. On day 2, the calvaria were washed in 1X PBS again and then placed in 2 ml of a collagenase solution (5.6 mM glucose, Mg²⁺/Ca²⁺-free PBS, Type 1 collagenase [Worthington Biochemical Corporation, Lakewood, NJ] at 230 units/ml) and shaken for 15 minutes at 37°C on a rotating platform to clean away any residual soft tissues and fibroblasts. The calvaria were moved to new wells and 2 ml of fresh collagenase solution and shaken continuously for an additional hour at 37°C. This suspension was passed through a cell strainer and centrifuged at 1000 RPM for 8 minutes. The cells were plated into 1 well of a 6-well plate in complete media and cultured to confluence. Media was changed every 2 to 3 days.

2.4 Cell Culture Conditions, Differentiation/Mineralization assays

For both MEFs and primary osteoblasts, cells were plated in 4-well plates (NUNC, Rochester, NY) coated in rat tail type I collagen (0.15 mg/ml) (BD Biosciences™, San Jose, CA) at 50,000 cells per well in complete media. The cells were allowed to settle and attach to the plate for 24 hours, then their media was changed to osteogenic media composed of α -MEM (Fisher Scientific, Pittsburgh, PA), 10% FBS, 1% Penn/Step, 5mM β -glycerophosphate, and 50 μ g/ml ascorbic acid. For the MEFs, media was supplemented or not with 100 ng/ml of BMP2 (R&D Systems,

Minneapolis, MN). Media was changed every 3 days. After 9 days of culture, alkaline phosphatase staining was performed according to the manufacturer's instructions (Chemicon International, Temecula, CA). After 12 days of culture, von Kossa staining was performed to assess mineral deposition. For this, cells were rinsed in 1X PBS and then fixed in 95% ethanol for 20 minutes at room temperature, then rinsed in dH₂O before being incubated in 5% (w/v) silver nitrate solution (Sigma) under ultra-violet light for 30 minutes. Mineral deposits were also assayed by Alizarin Red staining (LifeLine Cell Technologies, Frederick, MD). Cells were rinsed and fixed in the same way, and then the wells were allowed to dry before 2% Alizarin Red solution was added for 15 minutes at room temperature. The solution was removed and the well rinsed 3X before imaging.

2.5 Immunostaining for Perlecan

MEFs were plated on an eight-chambered glass microplate (NUNC) at 8,000 cells per well and, after 3 days of culture, were rinsed 3 times in 1X PBS and fixed for 10 minutes in methanol at 4°C. After another rinse, they were incubated and permeabilized for 1 hour in blocking buffer [10% (v/v) BSA, 0.15% (v/v) Tween 20 in Tris-buffered saline (TBS)]. They were immunostained with rabbit primary antibody against perlecan (1:100 dilution, LifeSpan Bioscience Inc., Seattle, WA) for one hour at room temperature, then rinsed 3 times in TBS-T. Secondary Alexa 488 conjugated goat anti-rabbit antibody (1:200 dilution, Invitrogen™, Carlsbad, CA) and Draq 5 (1:1000 dilution, Biostatus, Ltd, Shepshed Leicestershire, UK) were added to the rinsed cells for 1 hour in a humidified chamber at 37°C in the dark. After a final rinse

in PBS, the slides were imaged on a Zeiss multi-photon confocal microscope using a C-Apochromat 10x/0.45 water immersion objective (Zeiss, Inc, Thornwood, NY).

2.6 Reverse Transcriptase-PCR Analysis

Alongside cell staining, total RNA was extracted from trypsinized cell pellets using the RNeasy kit (Qiagen, Valencia, CA). mRNA extracts were DNase-treated using the DNA-freeTM DNase kit (Ambion, Austin, TX) to eliminate DNA contamination from the samples. cDNA was generated from mRNA samples using a reverse transcriptase polymerase chain reaction (RT-PCR) kit according to the manufacturer's instructions (Qiagen). An RT² Profiler PCR Array System (SABiosciences, Valencia, CA) was initially used to identify changes in osteogenesis in perlecan-deficient cells relative to WT cells. Perlecan-deficient and WT mRNA levels for selected mineralization markers were then quantitatively analyzed using real-time PCR (quantitative-PCR) with primers ordered through SABiosciences and using β -actin and glyceraldehyde 3-phosphate dehydrogenase (GAPDH) for standardization.

2.7 ELISA Analysis of Media

Media conditioned from cell culture was collected at the corresponding time points of mRNA extraction, centrifuged, and stored at -20°C. An osteocalcin ELISA was run with the samples for each condition according to the manufacturer's instructions (Biomedical Technologies Inc., Stoughton, MA).

Chapter 3

RESULTS

3.1 Differentiation/Mineralization Results in MEFs

3.1.1 Expression of Perlecan by Primary WT and Perlecan-Deficient MEFs

Primary MEFs from perlecan-deficient mice grown for nine days in a monolayer exhibited much less perlecan secretion than did WT cells when immunostained with an antibody against perlecan (Figure 5). Furthermore, perlecan in the mutant cells displayed a staining pattern that suggests the small amount of perlecan is retained intracellularly (Figure 5B). This primary culture model represents a good system in which to study the molecular consequences of perlecan deficiency in the matrix because it mirrors the *in vivo* expression pattern found in both WT and perlecan mutant cartilage matrices of strong extracellular staining in the WT cells vs. primarily intracellular signal in the perlecan-deficient cells.

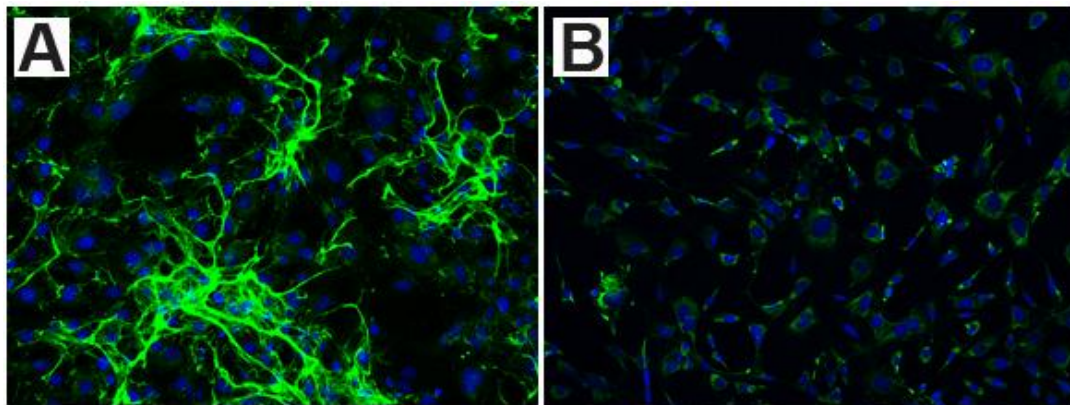


Figure 5. Perlecan immunostaining of WT and perlecan-deficient primary MEFs *ex vivo*. Perlecan is secreted by WT cells (Green, A) but only small amounts of perlecan, which are retained intracellularly, are expressed by perlecan-deficient cells (B). Cell nuclei are stained in blue.

3.1.2 Differentiation of MEFs with BMP2

Alkaline phosphatase staining was assayed as a marker of differentiation in MEFs cultured in osteogenic conditions for 9 days. When cultured in osteogenic media alone, WT and mutant cells exhibited little alkaline phosphatase activity. However, with the addition of 100 ng/ml of the growth factor BMP2, the perlecan-deficient cells exhibited much greater alkaline phosphatase activity than treated WT cells (Figure 6). This assay was repeated three times with similar results. Perlecan-deficient cells treated with BMP2 consistently displayed increased levels of alkaline phosphatase activity relative to both untreated cells and treated WT cells.

3.1.3 Mineralization Assay in Differentiated MEFs

Following differentiation of MEFs by BMP2 treatment as measured by increased alkaline phosphatase activity, the assay was extended to determine the cells' mineralization potential. After at least 12 days of culture under osteogenic conditions and in the presence or absence of BMP2, perlecan-deficient and WT cells were stained with silver nitrate to assay mineral nodule deposition and calcium content. The perlecan-deficient cells treated with growth factor were the only cells able to consistently form mineral deposits (Figure 7) that were associated with nodule formation in the cell layer. This experiment was repeated 3 times with similar results.

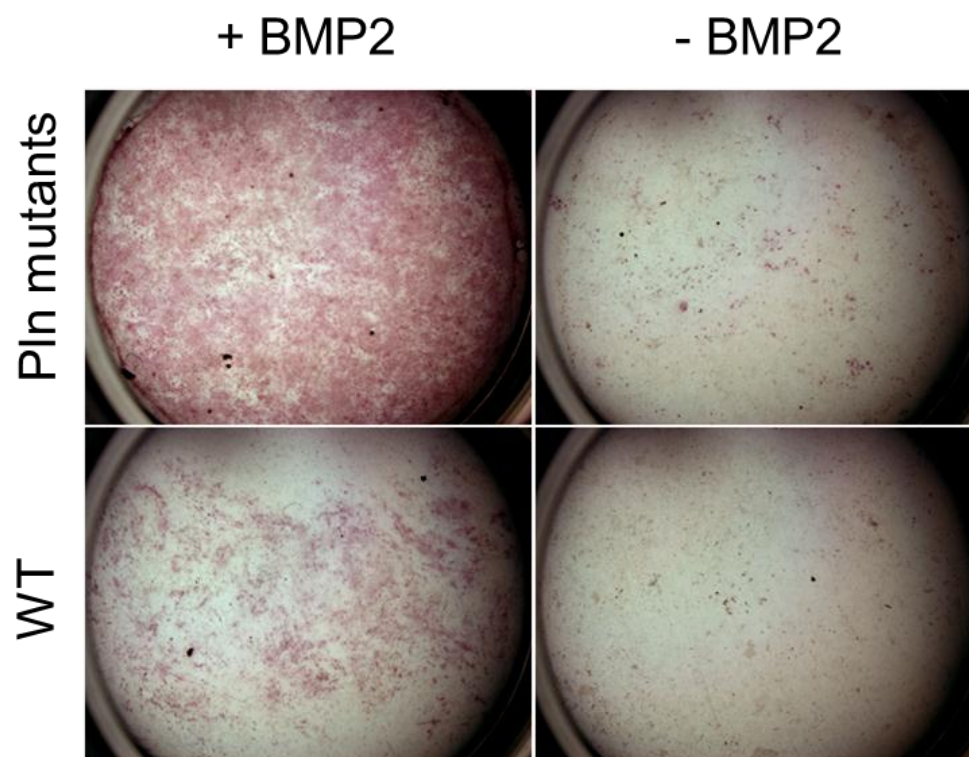


Figure 6. Alkaline phosphate staining is elevated in perlecan-deficient MEFs treated with BMP2 compared to treated WT MEFs. Little activity is seen in untreated cells of both genotypes.

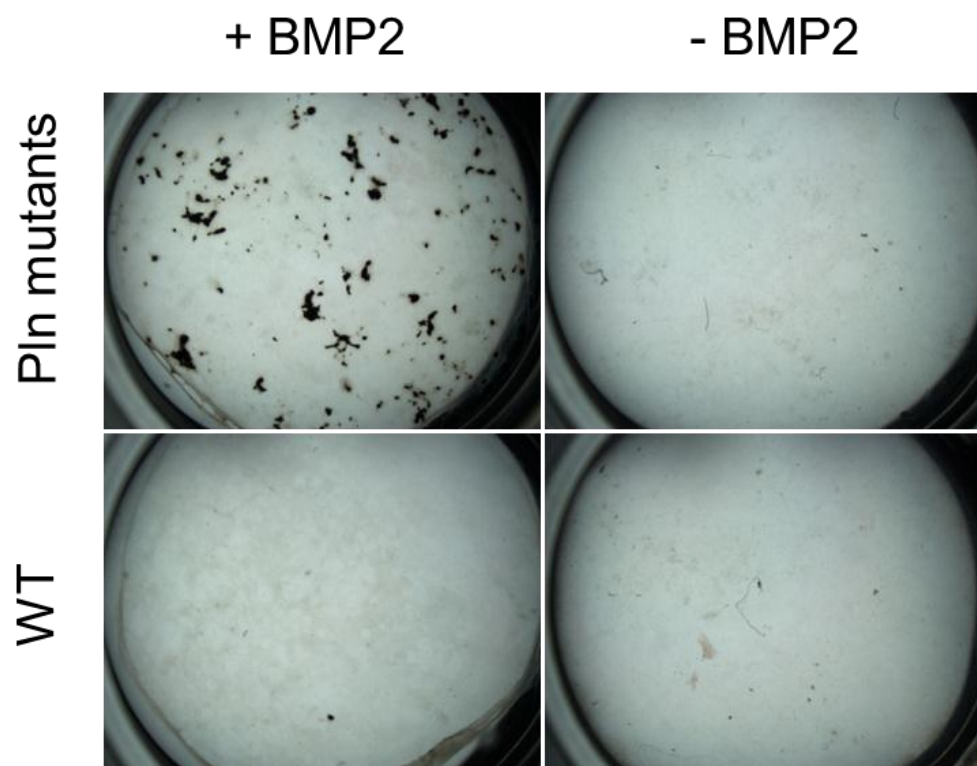


Figure 7. Von Kossa staining of WT and perlecan deficient MEFs only shows mineral deposition in the perlecan-deficient cells treated with BMP2.

3.1.4 Analysis of Mineralization Marker Gene Expression in Perlecan-Deficient MEFs Relative to WT

Relative amounts of mRNA of several markers of mineralization were quantitatively analyzed in both WT and perlecan-deficient MEFs treated with BMP2 at later stages of differentiation and mineralization using RT-PCR. Initially, an osteogenesis array system of RT-PCR was used to determine if any genes associated with the osteogenic pathway were upregulated as a result of perlecan deficiency (data not shown). Several genes were found to be upregulated in BMP2-treated perlecan-deficient cells versus WT cells treated for 12 days with BMP2. Alkaline phosphatase, for example, was upregulated over 38-fold in mutant cells, which is consistent with the staining seen in the cells at day 9 (Figure 6). Numerous genes involved in osteogenesis were increased more than twofold in BMP2-treated perlecan mutant MEFs versus WT. From the information gained from the array, RT-PCR was run on samples from additional differentiation assays. Figure 8 contains a summary of the results from three independent assays for the following selected markers: alkaline phosphatase (Alpl), osteocalcin (Bglap1), Phex, and Runx2. The values represent data from later time points during culture when mineralization was observed, ranging from day 12 to day 15. Although exact same relative fold change values at specific time points were not obtained, overall data was consistent between assay trials when equivalent mineralization states were compared.

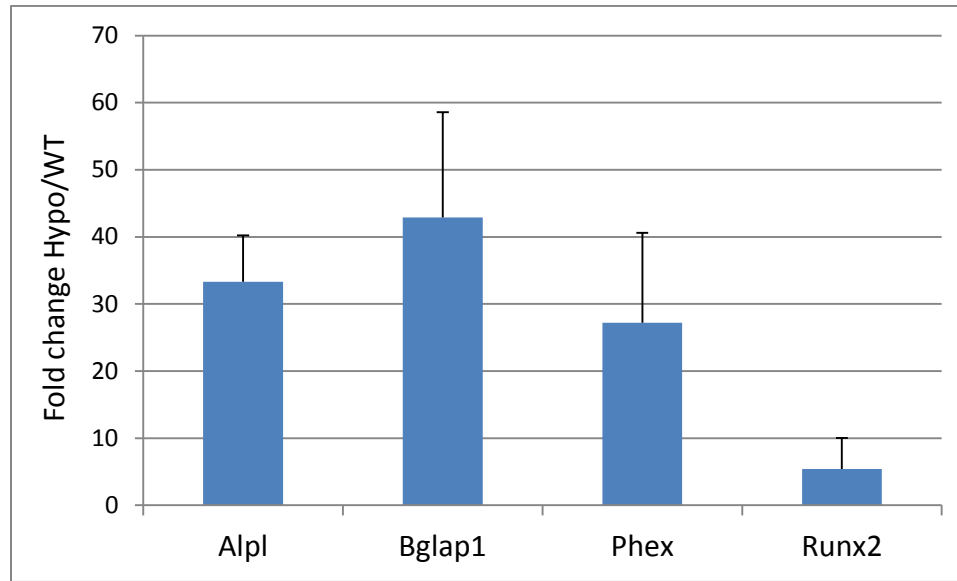


Figure 8. Quantitative real time PCR data for selected osteogenesis markers reveals significant upregulation in BMP2-treated perlecan-deficient cells relative to treated WT cells. RNA came from time points of culture in which mineral deposits were observed in the cell cultures. Alpl=alkaline phosphatase, Bglap1=bone gla protein 1 or osteocalcin, Phex=phosphate regulating endopeptidase homolog, X-linked, Runx2=transcription factor.

3.1.5 Perlecan-Deficient MEFs Secrete Elevated Levels of Osteocalcin Relative to WT During Mineralization

Levels of secreted osteocalcin (OCN) were assayed from conditioned media collected from MEFs during mineralization by ELISA assay. Osteocalcin, or bone Gla protein 1 (Bglap1), is secreted by osteoblasts and is an indicator of bone formation and remodeling (Lee, Hodges and Eastell 2000). Although osteocalcin concentrations differed considerably between trials due to experimental conditions, osteocalcin secretion in the media was greatly increased in BMP2-treated perlecan deficient cells relative to untreated mutant and both treated and untreated WT cells (Table 2). In the

last trial, the levels of secreted osteocalcin were too low to be detectable by ELISA when mineral nodules were barely visible using the von Kossa method. The only measurements where osteocalcin was detectable corresponded to media conditioned from perlecan-deficient cells in later stages of mineralization (day 15 and day 18), when nodule formation was visible to the eye and mineralization was confirmed by von Kossa staining. The secreted osteocalcin values at day 18 of culture averaged 533 ng/ml in media conditioned from perlecan-deficient cells treated with BMP2, which is on the same order as the results of the first trial and matches observed mineralization activity.

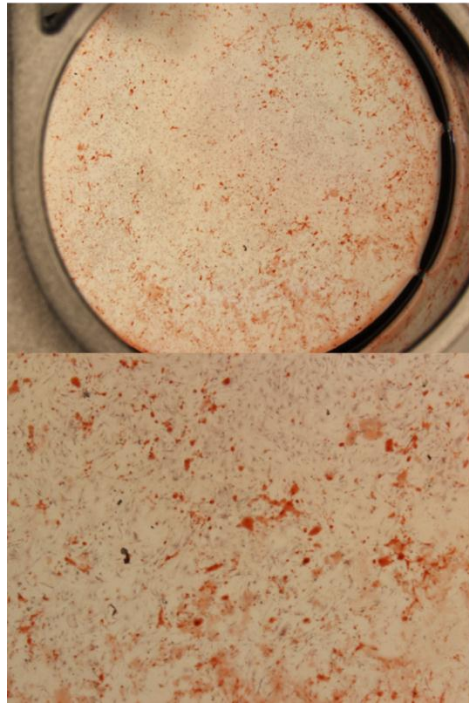
Table 2. Osteocalcin levels secreted into the media of WT and mutant MEFs culture in the presence or absence of BMP2. In both trials 1 and 2, media samples were pooled from different sample wells for the readings.

		OCN (ng/mL)	FOLD CHANGE
Trial 1 Media collected from culture d9-12	WT -BMP2	0.87	1
	WT +BMP2	1.92	2.2
	Pln def. -BMP2	0.91	1.0
	Pln def. +BMP2	247.47	284.4
Trial 2 Media collected from culture d9-12	WT -BMP2	0.98	1
	WT +BMP2	3.16	3.2
	Pln def. -BMP2	1.72	1.8
	Pln def. +BMP2	4899.66	4999.7

3.2 Mineralization Data in Primary Osteoblasts

Primary perlecan-deficient and WT calvarial osteoblasts seeded at approximately 20,000 cells per well in 4-well culture dishes exhibited comparable mineral deposits as assayed by Alizarin red staining (Figure 9). The osteoblasts were cultured for 21 days under osteogenic conditions. This assay was only performed once successfully due to difficulties in obtaining large enough quantities of perlecan mutant primary cell lines.

Perlecan-deficient Osteoblasts



WT Osteoblasts

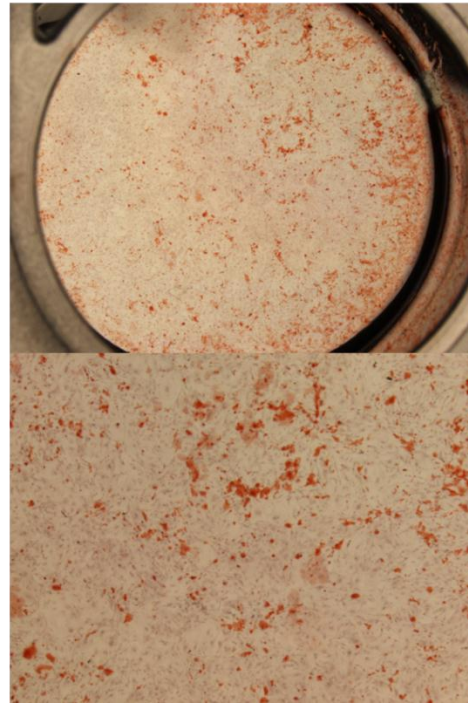


Figure 9. Perlecan-deficient and WT osteoblasts at day 21 of culture under osteogenic conditions exhibit similar patterns of Alizarin red staining.

Chapter 4

DISCUSSION

Based on our results, perlecan deficiency clearly potentiates the effect of BMP2 on differentiation and mineralization in primary MEFs in an *ex vivo* cell culture system, resulting in a distinct phenotype in perlecan mutant cells. When cultured under osteogenic conditions, the MEFs have poor intrinsic ability to differentiate. When BMP2 is added to the media of cells producing a perlecan-deficient matrix, enhanced differentiation and mineralization are observed by the cells. Alkaline phosphatase activity is generally accepted as a marker of osteoblast differentiation (Owen et al. 1990), and the greatest levels of activity are seen in perlecan-deficient cells treated with BMP2. Similarly, differentiation to the point of nodule formation and mineral deposition, visualized by von Kossa staining, was only seen in BMP2 treated perlecan-deficient cells when compared to all other conditions. Interestingly, alkaline phosphatase activity and mineral deposition occurred more suddenly than previously published in the literature (Owen et al. 1990), with mineral deposits visible in the perlecan-deficient cultures starting at day 12. This is indicative of rapid differentiation when perlecan is decreased in the extracellular matrix. When the perlecan-deficient MEFs were treated with BMP2, numerous markers of osteogenesis and mineralization were upregulated at the mRNA level, and they secreted much higher levels of osteocalcin in cell culture when compared with WT cells treated under the same conditions. Alkaline phosphatase and Phex are markers of osteoblast activity that cleave and regulate phosphate availability. Osteocalcin is a non-collagenous

protein found in bone produced by osteoblast, and is a marker of mineralization (Lee et al. 2000). Runx2 is the transcription factor associated with the early stages of osteoblast differentiation. Upregulation of these markers support the conclusion that enhanced osteogenesis occurs in perlecan-deficient primary cultures.

The data from the primary osteoblast assay appears consistent with our overall hypothesis (Figure 9), as both the WT and the perlecan-deficient osteoblasts mineralized to the same extent in culture. This model was chosen to represent a further stage of differentiation, a system in which cells are already committed to the osteoblast phenotype and are no longer as responsive to differentiation signals. The cells were cultured under osteogenic conditions but not treated with BMP2. No noticeable difference in mineralization was seen between the two phenotypes in the assay after 21 days of culture. In this experiment, however, we were forced to seed cells at a relatively low density for optimal osteoblast mineralization. This is due in part to an apparent lower proliferation potential of mutant vs. WT primary osteoblasts in culture, which resulted in a long waiting period between isolation and seeding for assessment of mineralization potential under equivalent culture conditions. For this reason, additional work using a different experimental approach is needed to confirm this preliminary data.

The definitive observations in the MEFs, though, suggest that the altered mineralization phenotype in mutant cells is due to the lack of interaction of heparin binding growth factors (HBGF) with perlecan in the ECM. Perlecan's heparan sulfate side (HS) chains are known to interact with soluble (HBGF) in the ECM, sequestering them and creating signaling gradients (Brown et al. 2008). In our proposed working model, perlecan's presence in the developing bone matrix serves to mediate proper

osteogenesis by regulating HBGF signaling, and more specifically, it accomplishes this through the interaction of the HS chains on domain I with HBGF. The HS chains may serve as a barrier for BMP2 signaling to osteoblast precursors by sequestering it from its cognate receptor (Bi et al. 2005). Decreased perlecan, and therefore fewer HS chains, in the matrix of perlecan-deficient MEFs results in the unregulated diffusion of BMP2 and allows for the altered differentiation and mineralization in culture. This can also explain the altered physiology of growth plates in perlecan-deficient mice (Figure 10). The decreased levels of perlecan and its HS chains (red symbol) in the cartilage of the developing growth plate of perlecan-deficient mice leads to enhanced growth factor diffusion through the matrix and signaling to osteoprogenitor cells (depicted in light blue). Decreased perlecan in the perichondrium will also lead to enhanced osteogenesis at the bone collar (Figure 11). This increase in the relative amount of differentiated osteoprogenitors and hypertrophic chondrocytes leads to the enlargement and disorganization of the growth plate seen in perlecan-deficient mouse bones (Figure 11). It cannot be excluded, however, that this phenotype may also be attributed to altered ECM organization in the absence of this large, scaffolding, matrix molecule. For instance, perlecan null mutations in mice result in the failure to remove the calcified cartilage matrix prior to vascular invasion during endochondral ossification (Ishijima et al. 2012), leading to the abnormalities in the growth plate and the complete lack of bone marrow space. In the perlecan-deficient model, where the skeletal defects are directly linked to lack of perlecan in the cartilage matrix rather than to deficiencies in blood vessel invasion (Lowe 2012), the growth plate phenotype is likely due to alterations of the matrix structure. In Figure 10, the red lines delineate the expansion of the terminal differentiation stage, indicated by increased collagen X

secretion in a perlecan-deficient mutant growth plate, relative to WT growth plates.

This phenomenon of increased calcification of the hypertrophic zone is consistent with histological data reported by another group in a perlecan null mutant model that results in perinatal lethality (Ishijima et al. 2012).

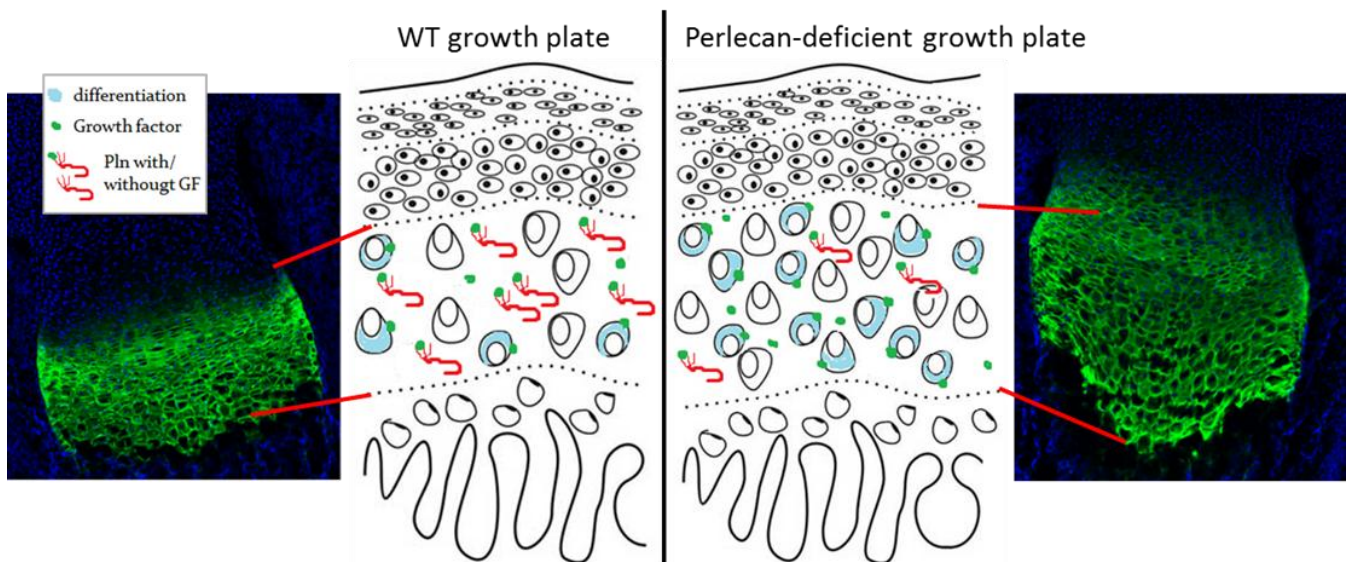


Figure 10. Working model of perlecan-deficiency's effect on bone development in the growth plate. Collagen X signal (green) delineates the hypertrophic zone in the growth plate. The perlecan-deficient hypertrophic zone is expanded, possibly due to either enhanced differentiation or ECM scaffolding defects, or both.

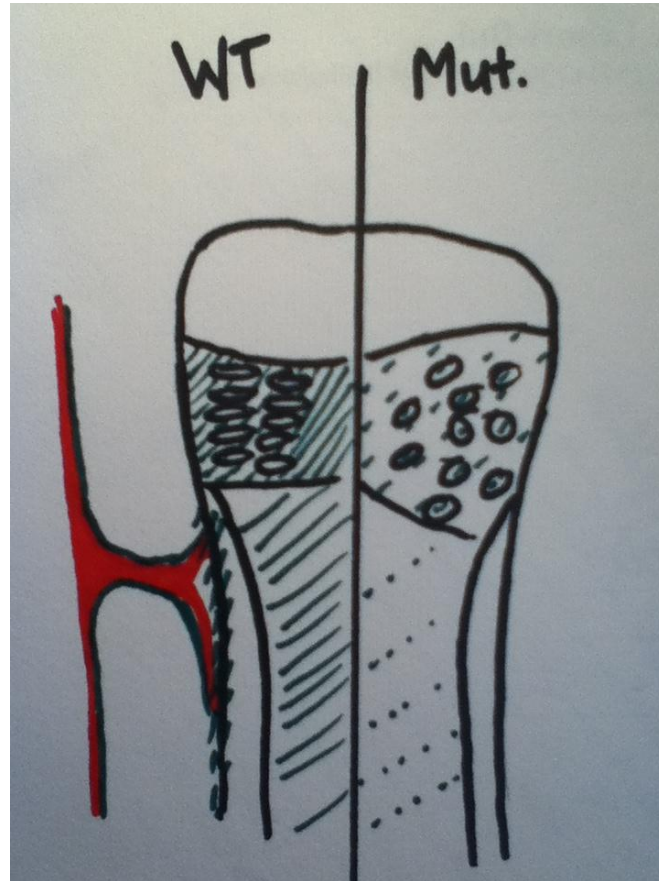


Figure 11. In the WT growth plate in developing bone, perlecan (green slashes) is expressed in the growth plate, periosteum, and bone marrow, where it serves to regulate osteogenesis for proper bone formation. In the perlecan mutant bone, its absence (broken green slashes) leads to unregulated signaling and differentiation, enlarged growth plate, and enhanced mineralization. The red structure on the left represents vascular invasion at the onset of endochondral ossification, which does occur in both the WT and perlecan-deficient bones although not pictured here.

In support of this model are similar phenotypic observations found in two other bone disease models resulting from loss-of-function mutations affecting HS synthesis and BMP signaling, hereditary multiple exostoses (HME, *Ext1* null mutations) and

fibrodysplasia ossificans progressiva (FOP, activating mutation of type I BMP receptor), respectively. *Ext1* is a glycosyltransferase located in the Golgi apparatus essential for polymerizing HS chains of HSPGs including perlecan. In our model, the HS chains' interaction with HBGF is crucial to the altered physiology of the bone matrix. Conditional ablation of *Ext1* was engineered in mice in the mesenchymal limb buds during development (Matsumoto et al. 2010). Although cartilage ECM organization will differ from our model because the perlecan core protein is not mutated in *Ext1* mice, the lack of HS in these mice is also expected to affect HBGF signaling. These mice have limb defects similar to the perlecan-deficient mice, including shortened long bones and expanded growth plates, as well as a greater distribution of BMP signaling domains in the developing bone (Matsumoto et al. 2010). Mutation of *Ext1* causes hereditary multiple exostoses (HME), which is characterized by abnormal mineralized outgrowths from the growth plate during development due to disorganization of the cartilage ECM (Zak, Crawford and Esko 2002). These observations of abnormal mineralization events during development support our model's proposed mechanism that the HS chains of perlecan are paramount in regulating osteogenesis.

FOP is a relatively rare, autosomal dominant, genetic disease in which a mutation in the *ACVRI* gene, which codes for the BMP type I receptor, results in a constitutively active receptor (Medicine 2007, Kaplan et al. 2011). This condition parallels the enhanced BMP signaling proposed in our perlecan-deficient model, but the result is much more severe in FOP. FOP patients suffer from drastic heterotopic bone formation in muscle and connective tissues such as ligaments and tendons, which leads to progressive loss of mobility and other serious, life-threatening complications.

Though perlecan deficiency results in a much milder phenotype than FOP, the similarity in phenotypes between these disorders supports the implication that increased signaling to BMP receptors leads to increased and aberrant bone formation activity, and is in support of our model for perlecan's role in regulating this function.

The results from this study strongly support the hypothesis that perlecan directly influences growth factor activity in developing bone tissue. While our proposed model of perlecan's HS chains interacting with HBGFs in developing bone matrix is strongly supported by other disease models such as HME and FOP, further experiments would expand on the mechanism underlying perlecan's role in endochondral ossification. Treatments with heparanase for example, to impair perlecan's HS chains' interaction with BMP2 in a differentiation/mineralization assay would shed light on the mechanism of perlecan HS chains' interaction with HBGFs. Hypothetically, the heparanase treatment should cause the WT cells' phenotype to resemble the altered mineralization seen in perlecan-deficient MEFs due to the loss of growth factor sequestration. Alternately, treatment with a HS-decorated perlecan domain I should rescue the abnormally high mineralization potential of perlecan-deficient osteoprogenitors and reverse their phenotype back to that of the WT cells by introducing growth factor regulation via HS-dependent binding mechanisms.

Data from our experiments demonstrates a marked increase in osteogenic potential for precursor cells present in a perlecan-deficient environment. As aforementioned, endochondral ossification depends on proper formation and organization of the cartilage anlagen prior to bone formation. Early on during endochondral ossification, it is possible that perlecan-deficiency has a similar enhancing effect on chondrogenesis. Wild-type perlecan is abundant in the

pericellular space of chondrocytes and mesenchymal progenitors. The enhanced osteogenesis resulting from perlecan-deficiency could very well be in conjunction with enhanced chondrogenesis afforded by the mutation by an identical mechanism of HBGFs interaction with HS chains present on the perlecan core protein. Both of these altered processes would then contribute to the development of abnormal bone.

Although our model proposes a developmental explanation for the altered bone phenotype seen with perlecan deficiency, adult mutant mouse bones do exhibit physiological differences from WT bones (Lowe et al. 2012). Mutant mouse bones have the aforementioned increased BMD, which may be explained by the organizational changes in the growth plate during bone development. However, this difference in BMD is sustained during remodeling throughout the adult life of the mouse, suggesting further regulation of mineralization events by perlecan during adulthood. An alternate hypothesis for perlecan's function in these regions is that the negatively charged HS chains inhibit mineralization directly by binding up free cations such as calcium in the matrix. Of note for this postulate is the observation that the LCS's width is significantly decreased in perlecan mutant cortical bone relative to WT. Furthermore, the LCS in WT mouse bones is approximately 78 nm in width, and perlecan, at 100-200 nm in length, is the only proteoglycan large enough to span the space's width (Thompson et al. 2011). Interestingly, perlecan present in the LCS of adult bone was proposed to act as a physical barrier or inhibitor mineralization. A further function proposed for perlecan in the LCS is contributing to mechanotransduction by cortical osteocytes (Thompson 2010). Perlecan presence in the pericellular matrix of LCS osteocytes suggests that it may sense the fluid flow around cortical osteocytes and plays an important function in both establishment and

maintenance of bone health. By interacting with an auxiliary subunit of T-type voltage-sensitive-calcium-channels (VSCCs) through a shared potential binding motif on the subunit and perlecan's domain III, perlecan may add to the regulation of the channels' activation, and subsequent intracellular calcium signaling. Though the suspected binding domain is thought to be on the core protein of perlecan, the long, extended HS chains may also provide important flow sensing in the LCS. This data, along with perlecan's large size and diverse domains, are strong evidence for structural or scaffolding functions of perlecan in the LCS, where it is abundant in WT mice. The mechanisms of perlecan's numerous apparent functions are not well understood, but it seems to affect bone morphology both during development and during remodeling throughout adult life.

In conclusion, our results show that severe reduction of perlecan, a HS proteoglycan abundant in cartilage and the periosteum, is associated with increased osteogenesis and an enhanced bone mineralization phenotype. The cell culture model of MEFs provides a useful and malleable tool for studying perlecan's function as a regulator of mineralization through the regulation of growth factor signaling. A greater understanding of this mechanism will lead to many potential clinical applications in musculoskeletal systems, for example, in the prevention and treatment of abnormal mineralization. Ectopic calcification can arise from several different sources, from genetic conditions such as FOP to events surrounding musculoskeletal injury or trauma. In osteoarthritis, abnormal growth and changes in subchondral bone as a result of cartilage degradation are a common occurrence and result in the loss of mobility and pain. Each of these disease examples involves bone formation processes which recapitulate the forces at work during early development. They involve

signaling and differentiation which lead to the initiation and growth of bone tissue outside of the skeleton, where it is debilitating and inappropriate for healthy function. A more comprehensive picture of how and why these mineralization events come about, and furthermore, perlecan's role in their control, will allow for novel treatments of these conditions.

REFERENCES

- Arikawa-Hirasawa, E., H. Watanabe, H. Takami, J. R. Hassell & Y. Yamada (1999) Perlecan is essential for cartilage and cephalic development. *Nat Genet*, 23, 354-8.
- Bi, Y., C. H. Stuelten, T. Kilts, S. Wadhwa, R. V. Iozzo, P. G. Robey, X. D. Chen & M. F. Young (2005) Extracellular matrix proteoglycans control the fate of bone marrow stromal cells. *J Biol Chem*, 280, 30481-9.
- Brown, A. J., M. Alicknavitch, S. S. D'Souza, T. Daikoku, C. B. Kirn-Safran, D. Marchetti, D. D. Carson & M. C. Farach-Carson (2008) Heparanase expression and activity influences chondrogenic and osteogenic processes during endochondral bone formation. *Bone*, 43, 689-99.
- Chen, D., M. Zhao & G. R. Mundy (2004) Bone morphogenetic proteins. *Growth Factors*, 22, 233-41.
- Cohn, D. H. (2001) Defects in extracellular matrix structural proteins in the osteochondrodysplasias. *Novartis Found Symp*, 232, 195-210; discussion 210-2.
- Costell, M., E. Gustafsson, A. Aszódi, M. Mörgelin, W. Bloch, E. Hunziker, K. Addicks, R. Timpl & R. Fässler (1999) Perlecan maintains the integrity of cartilage and some basement membranes. *J Cell Biol*, 147, 1109-22.
- Cummings, B. 2006. Diagram of endochondral ossification. Endochondral ossification diagram. Pearson Education, Inc.
- Frattini, A., P. Vezzoni, A. Villa & C. Sobacchi (2007) The Dissection of Human Autosomal Recessive Osteopetrosis Identifies an Osteoclast-Poor Form due to RANKL Deficiency. *Cell Cycle*, 6, 3027-3033.
- Ishijima, M., N. Suzuki, K. Hozumi, T. Matsunobu, K. Kosaki, H. Kaneko, J. R. Hassell, E. Arikawa-Hirasawa & Y. Yamada (2012) Perlecan modulates VEGF signaling and is essential for vascularization in endochondral bone formation. *Matrix Biol*, 31, 234-45.

- Jiang, X. & J. R. Couchman (2003) Perlecan and tumor angiogenesis. *J Histochem Cytochem*, 51, 1393-410.
- Kaplan, F. S., V. Y. Lounev, H. Wang, R. J. Pignolo & E. M. Shore (2011) Fibrodysplasia ossificans progressiva: a blueprint for metamorphosis. *Ann N Y Acad Sci*, 1237, 5-10.
- Katagiri, T., A. Yamaguchi, M. Komaki, E. Abe, N. Takahashi, T. Ikeda, V. Rosen, J. M. Wozney, A. Fujisawa-Sehara & T. Suda (1994) Bone morphogenetic protein-2 converts the differentiation pathway of C2C12 myoblasts into the osteoblast lineage. *J Cell Biol*, 127, 1755-66.
- Kelley, B. P., F. Malfait, L. Bonafe, D. Baldrige, E. Homan, S. Symoens, A. Willaert, N. Elcioglu, L. Van Maldergem, C. Verellen-Dumoulin, Y. Gillerot, D. Napierala, D. Krakow, P. Beighton, A. Superti-Furga, A. De Paepe & B. Lee (2011) Mutations in FKBP10 cause recessive osteogenesis imperfecta and Bruck syndrome. *J Bone Miner Res*, 26, 666-72.
- Kirn-Safran, C. B., R. R. Gomes, A. J. Brown & D. D. Carson (2004) Heparan sulfate proteoglycans: coordinators of multiple signaling pathways during chondrogenesis. *Birth Defects Res C Embryo Today*, 72, 69-88.
- Knox, S. M. & J. M. Whitelock (2006) Perlecan: how does one molecule do so many things? *Cellular and Molecular Life Sciences*, 63, 2435-2445.
- Lee, A. J., S. Hodges & R. Eastell (2000) Measurement of osteocalcin. *Ann Clin Biochem*, 37 (Pt 4), 432-46.
- Lowe, D. 2012. Angiogenesis in WT vs. Pln-deficient mice. ed. N. Lepori-Bui.
- Lowe, D., P. Fomin, N. Lepori-Bui, L. Sloofman, X. Zhou, M. Farach-Carson, L. Wang & C. Kirn-Safran. 2012. Deficiency in Perlecan/HSPG2 during Cartilage Growth Plate Development Enhances Osteogenesis and Decreases Quality of Adult Bone in Mice.
- Matsumoto, Y., K. Matsumoto, F. Irie, J. Fukushi, W. B. Stallcup & Y. Yamaguchi (2010) Conditional ablation of the heparan sulfate-synthesizing enzyme Ext1 leads to dysregulation of bone morphogenic protein signaling and severe skeletal defects. *J Biol Chem*, 285, 19227-34.
- Medicine, U. S. N. L. O. 2007. Fibrodysplasia ossificans progressiva. Genetic Home Reference.

- Olsen, B. R., A. M. Reginato & W. Wang (2000) Bone development. *Annu Rev Cell Dev Biol*, 16, 191-220.
- Owen, T. A., M. Aronow, V. Shalhoub, L. M. Barone, L. Wilming, M. S. Tassinari, M. B. Kennedy, S. Pockwinse, J. B. Lian & G. S. Stein (1990) Progressive development of the rat osteoblast phenotype in vitro: reciprocal relationships in expression of genes associated with osteoblast proliferation and differentiation during formation of the bone extracellular matrix. *J Cell Physiol*, 143, 420-30.
- Rodgers, K. D., T. Sasaki, A. Aszodi & O. Jacenko (2007) Reduced perlecan in mice results in chondrodysplasia resembling Schwartz-Jampel syndrome. *Hum Mol Genet*, 16, 515-28.
- Rosen, V. 2012. Osteoblast sensitivity to BMP2. ed. N. Lepori-Bui.
- Sobacchi, C., A. Frattini, M. M. Guerrini, M. Abinun, A. Pangrazio, L. Susani, R. Bredius, G. Mancini, A. Cant, N. Bishop, P. Grabowski, A. Del Fattore, C. Messina, G. Errigo, F. P. Coxon, D. I. Scott, A. Teti, M. J. Rogers, P. Vezzoni, A. Villa & M. H. Helfrich (2007) Osteoclast-poor human osteopetrosis due to mutations in the gene encoding RANKL. *Nat Genet*, 39, 960-2.
- Steiner, R., M. Pepin & P. Byers. 2005. Osteogenesis Imperfecta. eds. R. Pagon, T. Bird, C. Dolan & e. al. Internet: GeneReviews.
- Thompson, W. R. 2010. Perlecan Modulates the Function of the Osteocyte Lacuno-Canalicular System. In *Biomechanics and Movement Science*, 222. University of Delaware.
- Thompson, W. R., S. Modla, B. J. Grindel, K. J. Czymmek, C. B. Kirn-Safran, L. Wang, R. L. Duncan & M. C. Farach-Carson (2011) Perlecan/Hspg2 deficiency alters the pericellular space of the lacunocanalicular system surrounding osteocytic processes in cortical bone. *J Bone Miner Res*, 26, 618-29.
- Tsumaki, N. & H. Yoshikawa (2005) The role of bone morphogenetic proteins in endochondral bone formation. *Cytokine Growth Factor Rev*, 16, 279-85.
- Whitelock, J. M. & R. V. Iozzo (2005) Heparan sulfate: a complex polymer charged with biological activity. *Chem Rev*, 105, 2745-64.
- Yamaguchi, A., T. Komori & T. Suda (2000) Regulation of osteoblast differentiation mediated by bone morphogenetic proteins, hedgehogs, and Cbfa1. *Endocr Rev*, 21, 393-411.

Zak, B. M., B. E. Crawford & J. D. Esko (2002) Hereditary multiple exostoses and heparan sulfate polymerization. *Biochim Biophys Acta*, 1573, 346-55.

Appendix

PERMISSION LETTER


**University of Delaware
Institutional Animal Care and Use Committee
Application to Use Animals in Research and Teaching**

(Please complete below using Arial, size 12 Font.)

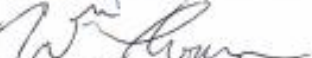
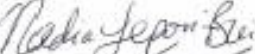


Title of Protocol: Transgenic Models of Skeletal and Metabolic Diseases	
AUP Number: 1204-2010-0	← (4 digits only — if new, leave blank)
Principal Investigator: Catherine B. Kim-Safran	
Common Name: Mice	
Genus Species: Mus Musculus	
Category Assigned: (please mark one) <input checked="" type="checkbox"/> A. None to slight or momentary pain or distress <input type="checkbox"/> B. Pain or distress will be alleviated by drugs or other means <input type="checkbox"/> C. Pain or distress will not be alleviated	

Official Use Only IACUC Approval Signature: <u>Steven D Brown</u> Date of Approval: <u>10 August 2009</u>
--

SIGNATURE(S) OF ALL PERSONS LISTED ON THIS PROTOCOL

I certify that I have read this protocol, accept my responsibility and will perform only the procedures that have been approved by the IACUC.

Name	Signature
1. Catherine Kim-Safran	
2. Padma Pradeepa Srinivasan	
3. William Thompson	
4. Peter Fomin	
5. Nadia Lepori-Bui	
6. Dylan Lowe	
7. Kerry Falgowski	
8.	
9.	
10.	
11.	
12.	
13.	
14.	
15.	